

Influence of removing the PMMA residues on surface of CVD graphene using contact-mode atomic force microscope

Woosuk Choi, Muhammad Arslan Shehzad, Sanghoon Park, Yongho Seo*

*Department of Nanotechnology and Advanced Material Engineering, and Graphene
Research Institute, Sejong University, Seoul, 143-747, Korea*

Contents

Figure S1: The photo lithographic procedure to make a sample for transport measurement

Figure S2: Damaged graphene in cleaning process when the normal force of AFM tip was excessively high.

Figure S3: Cleaning results for exfoliated graphene surfaces.

Figure S4 : Raman mapping images of graphene surface for G and 2D peak before and after the AFM cleaning.

Figure S5: Transconductance data measured for four different FET devices based on CVD graphene.

Figure S6: Comparison between cleaning efficiencies in vertical and horizontal scanning directions.

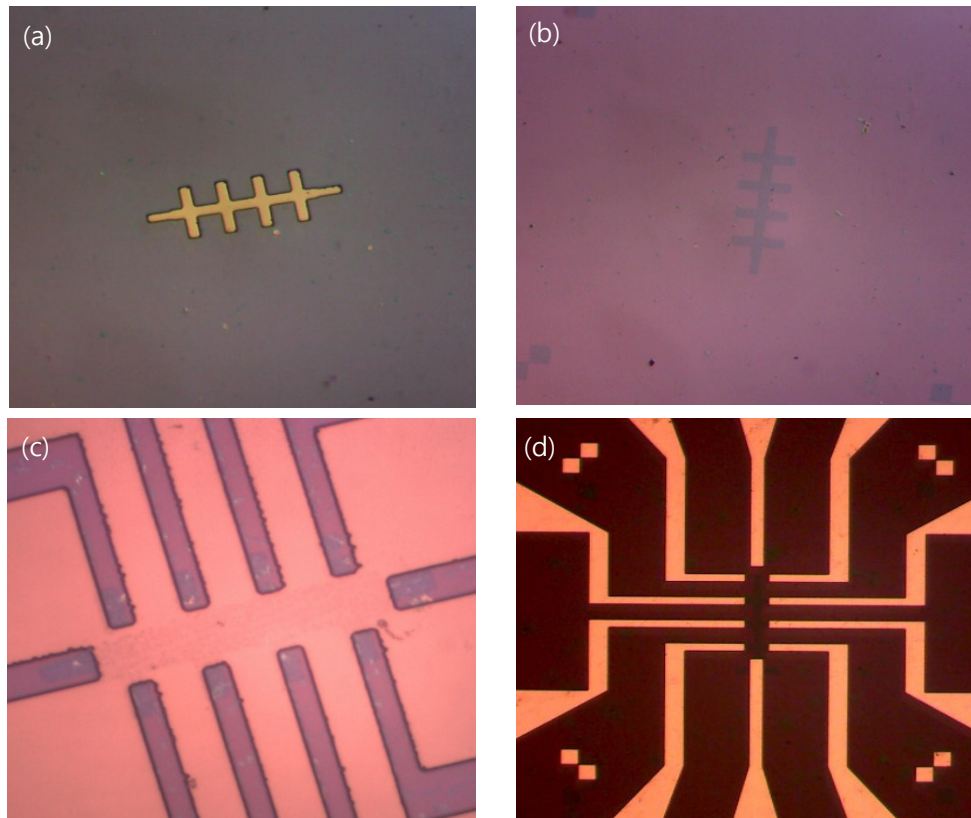


Figure S1 Photographic images of representative graphene sample. Photolithography was performed to fabricate the Hall bar pattern. The optical microscopic images were taken after development (a), after RIE (b), after 2nd photo lithography (c) and after lift-off (d).

For the photolithography, the photo resist (AZ GXR-601) was coated by a spinner on the sample. The spin-coating procedure was step1 (500 rpm, 5 s) and step2 (4000 rpm, 40 s), and it was baked at 90 °C for 1 min. The UV exposure dose was about W meter: 200, A/V meter: 4.2 for 4 sec to make hall bar patterns. It was developed using AZ 300MIF developer for 1 minute, and rinsed in deionized (DI) water. (Fig. S1a)

RIE was performed using O₂ plasma for 3 s to etch the graphene, and the sample was rinsed by acetone to remove photoresist. Figure S1b shows photographic image of the sample after removing PMMA by acetone. The second photolithography was performed again for the Au electrode. Figure S1c shows the aligned state of the lithography. Ti/Au (5/50 nm) electrodes were deposited using an e-beam evaporator (KOREA VACUUM TECH, KVE-E4006). After lift-off process (Fig. S1d), transport measurement of graphene device was carried out.

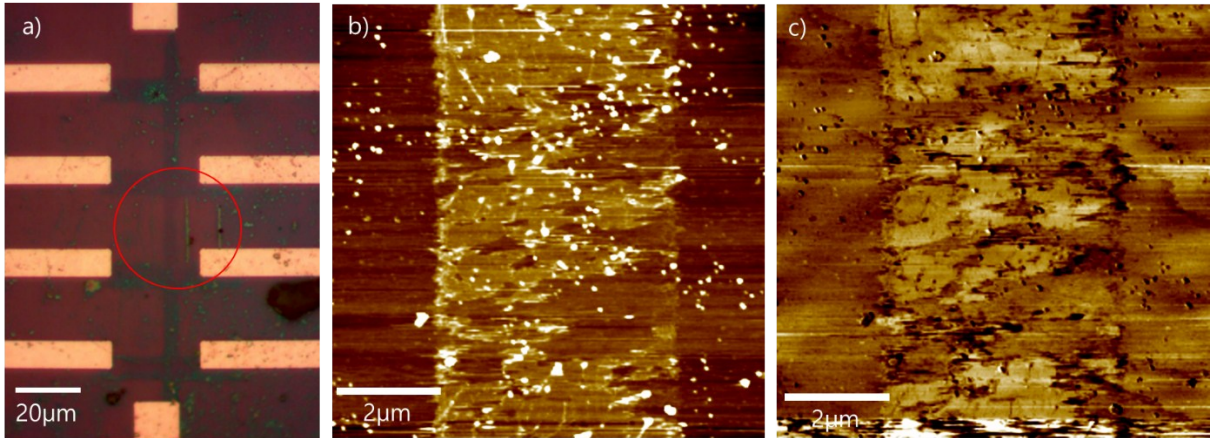


Figure S2: unsuccessful cleaning result when normal force of AFM tip was excessively high (~ 30 nN). (a) Optical microscope image of the device was taken, after it was cleaned. These topographic (b) and lateral force (c) images obtained during cleaning process, show that sample was damaged via scanning.

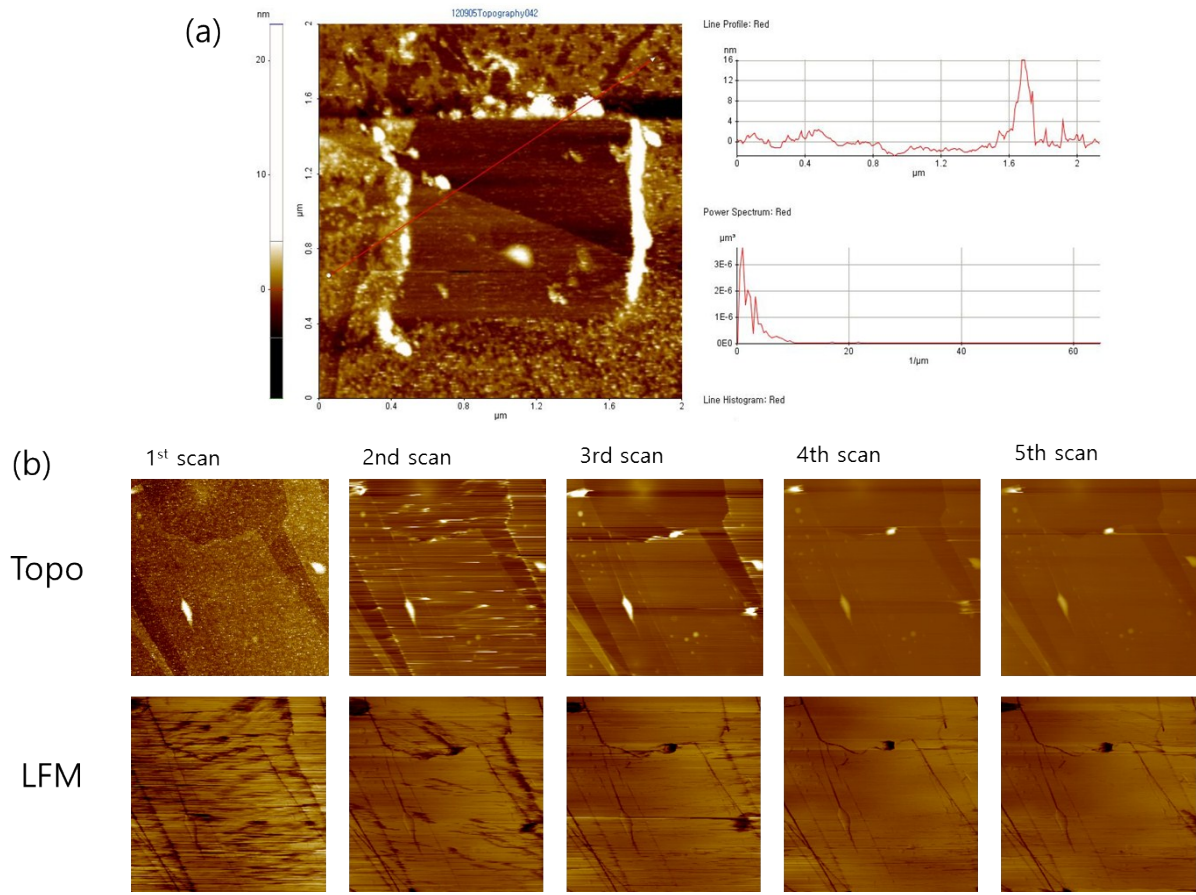


Figure S3: (a) The AFM image and line profile show cleaned surface of an exfoliated graphene after AFM scanning. (b) Repeated scanning process was monitored by AFM scanning for an exfoliated graphene on top of hBN substrate. Topographic (top) and lateral force (bottom) images show that the surface of graphene was cleaned gradually.

PMMA (950, A2 from MicroChem Inc.) and Scotch tape (3M Inc.) were used for transferring to the hBN substrate. After the transfer, acetone was used to remove the chemicals from the PMMA and Scotch tape.

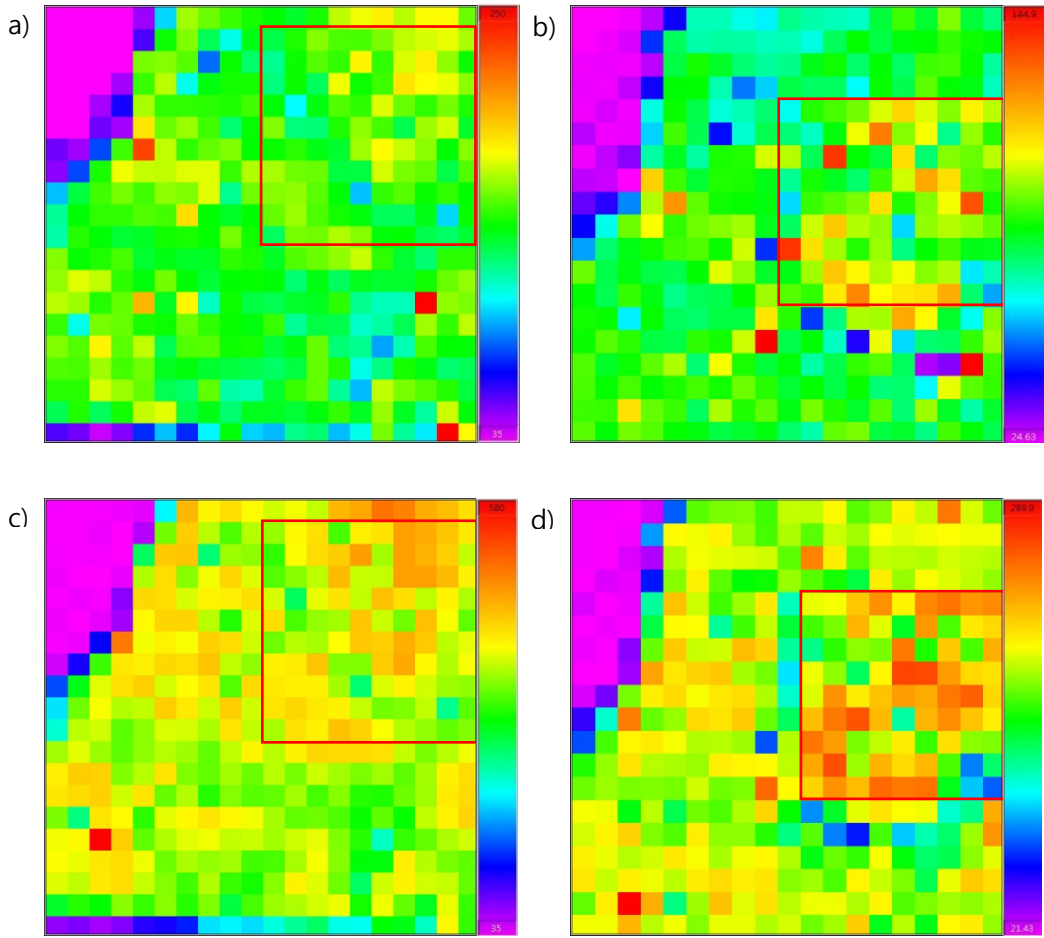


Figure S4 Raman mapping images of graphene surface for G (a) and 2D (c) peak before the AFM cleaning, for G (b) and 2D (d) peak after the AFM cleaning. The red square area indicates the area where AFM cleaning was performed.

Figures S4 show Raman mapping images of graphene surface for G (a) and 2D (c) peak before the AFM cleaning, for G (b) and 2D (d) peak after the AFM cleaning. The red square area indicates the area where AFM cleaning was performed. In this figure, the states of the laser source before and after AFM cleaning were changed, the data cannot be compared directly. Therefore, the cleaning effect can be confirmed by investigating the Raman mapping images before and after the AFM cleaning and comparing the Raman data between the cleaned and uncleaned areas. It was confirmed that the relative average intensities on cleaned area, compared with surrounding area were increased about 5% and 7% for G and 2D peaks, respectively.

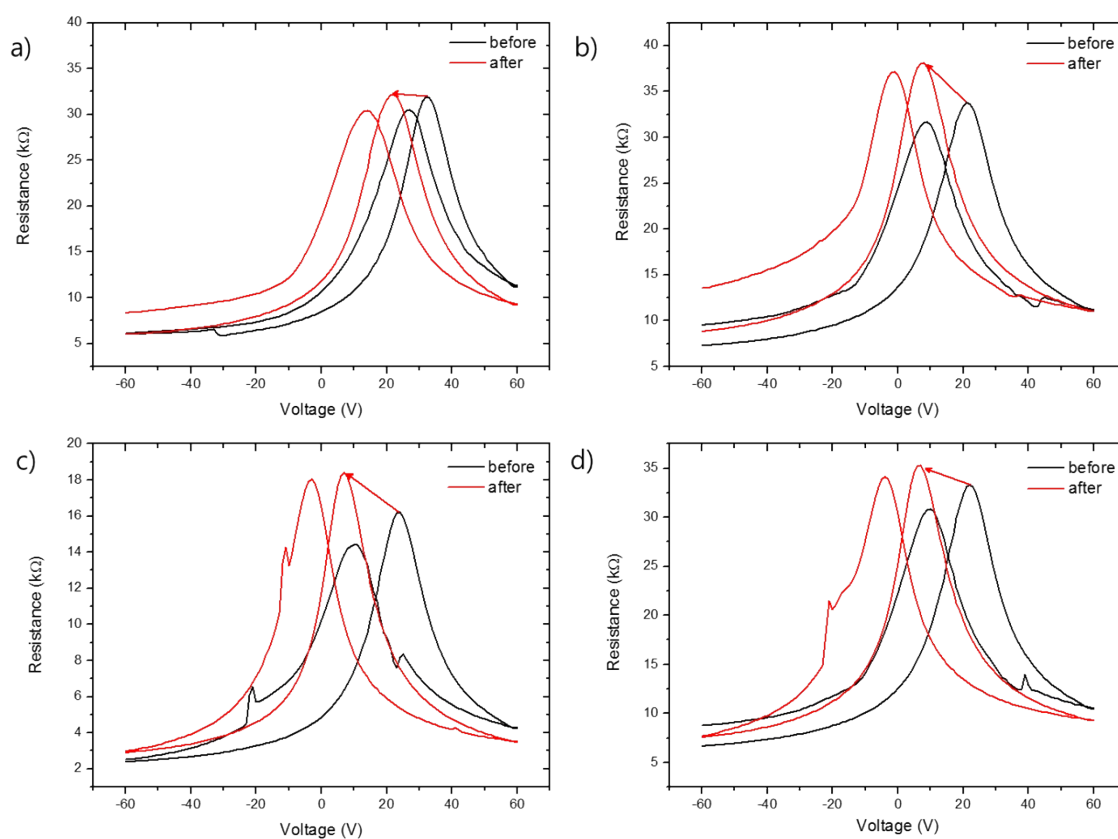


Figure S5: (a-d) Transconductance data were measured for four different FET devices based on CVD graphene, respectively. These devices showed hysteresis behaviors and abnormal peaks due to unintended charging for repeated cycling, but the Dirac peak shifts are clear.

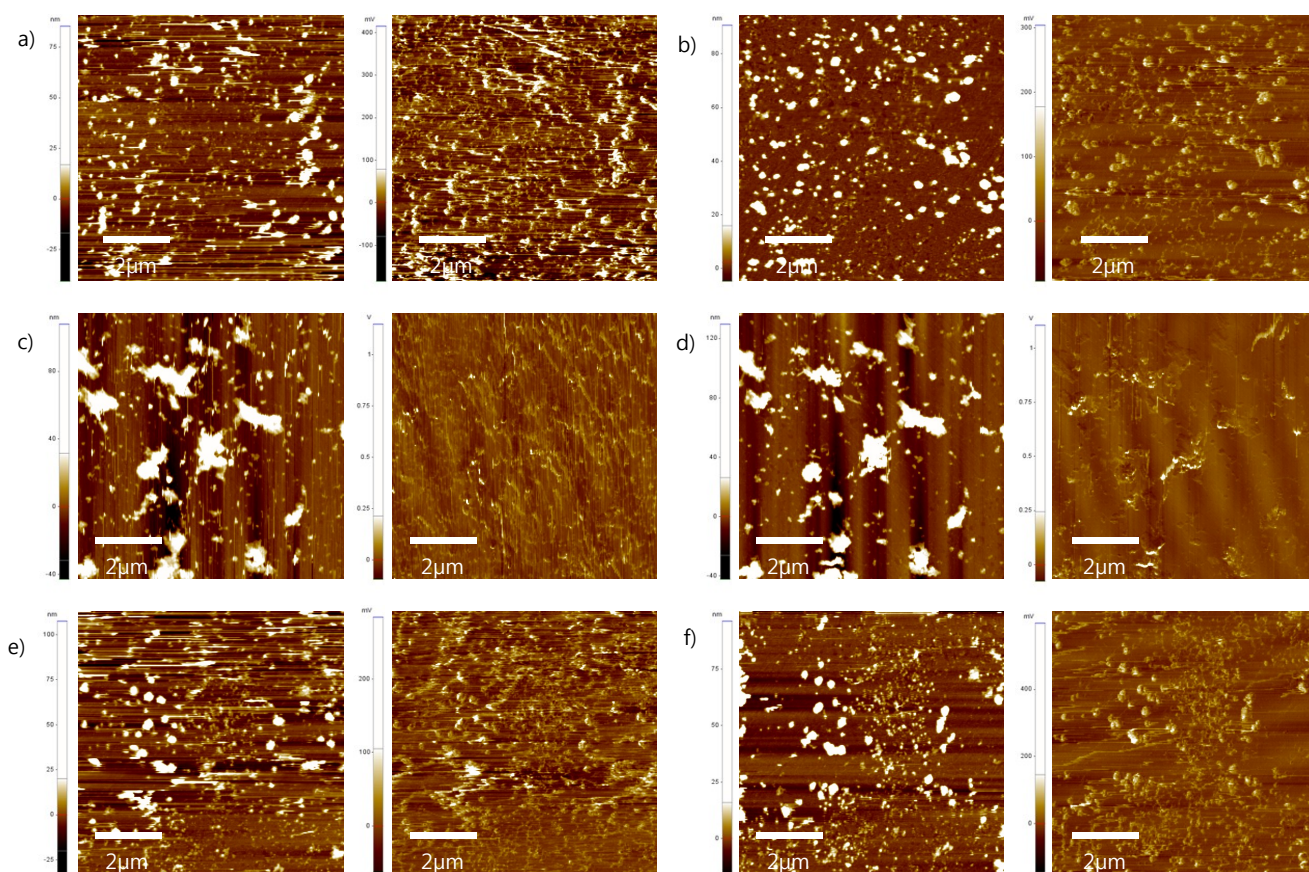


Figure S6 The AFM images show topography (left) and LFM image (right) of AFM cleaning in 0° (horizontal) before (a) and after (b), in 90° (vertical) before (c) and after (d), respectively. (e-f) The AFM images are topography (left) and LFM image (right) of AFM cleaning by alternating directional scans before and after cleaning, respectively.

The image of Figure S6 (a-b) is topography (left) and LFM image (right) before (a) and after (b) AFM cleaning in horizontal direction. The scanning conditions were similar to the previous experiment. (Scan speed: 0.2 Hz, set point: 15 nN, cantilever: Multi75DLC (force constant: 3N/m)) Vertical scanning (Fig. R4 (c-d)) shows a slightly better cleaning effect compared to horizontal scanning. Comparing images before and after, it can be seen that the residues were slowly removed and became cleaner, except for large chunks. This can also be seen more clearly in the right LFM image. In the horizontal scan, the root mean surface roughness value decreased from 8.805 nm to 6.836 nm, and in the vertical scan it decreased from 15.79 nm to 12.69 nm, slightly more than the horizontal scan. These results show that

vertical scans are more effective than horizontal scans. On the other hand, the images of Fig. S6 (e, f) are AFM topography (left) and LFM image (right) before and after AFM cleaning, when it was scanned in alternating directions. This result are also similar to the vertical scan. These experimental results suggest that the angle of scan affects the cleaning effect, due to the anisotropic shape of the cantilever. These results are included in the supplementary Fig. S6.